Available online at www.sciencedirect.com
ScienceDirect
Electric Power Systems Research 77 (2007) 155–162
ELECTRIC POWER SYSTEMS RESEARCH
www.elsevier.com/locate/epsr

Islanding detection of grid connected distributed generators using TLS-ESPRIT

H.H. Zeineldin *, T. Abdel-Galil, E.F. El-Saadany, M.M.A. Salama

Department of Electrical and Computer Engineering, University of Waterloo, Waterloo, Ont., Canada N2L 3G1

Received 28 March 2005; received in revised form 14 February 2006; accepted 17 February 2006
Available online 3 April 2006

Abstract

A critical protection requirement for grid connected distributed generators (DG) is anti-islanding protection. In this paper, a new islanding detection method is proposed based on monitoring the generator's frequency. Two new features, the frequency of oscillation and the damping factor of the generator's frequency output waveform, are extracted using the total least square-estimation of signal parameters via rotational invariance techniques (TLS-ESPRIT) algorithm. The proposed method has been tested under various scenarios such as load change, short circuit, and capacitor switching.

Keywords: Distributed generation; Islanding detection; Fault currents; Power distribution

1. Introduction

Despite the favorable aspects grid-connected DGs can provide to the distribution system, a critical demanding concern is islanding detection and prevention. Islanding is a condition where the DG supplies power and is not under the direct control of the utility. According to the IEEE Std. 929-2000, such situation should be prevented due to several reasons concerning personnel safety, power quality and safe operation of the DG and distribution system. In general, islanding detection methods are classified into two main groups: active and passive methods [1].

Active islanding detection methods interact with the system operation. This could be done by injecting a distorted current waveform, using a frequency pattern, or by varying the output power of the DG continuously. Island loading for which the islanding detection method fails to detect islanding is known as the nondetection zone (NDZ). Despite that active methods are characterized by small NDZ, active methods affect the power quality of the distribution system. They are most commonly applied to inverter based DGs. Active methods include active frequency drift (AFD), output power variation, slip mode frequency shift (SMFS), and etc. [2–4].

Passive islanding detection techniques depend on measuring system parameters and setting thresholds for the measurable parameters. Passive islanding detection methods can be applied to any type of dispersed generation whether the DG is of the synchronous type or the inverter based type. The main challenge when designing a passive islanding detection method is to choose the most significant parameter and its threshold value to detect islanding for almost all loadings while avoiding nuisance tripping. Thresholds are chosen such that the islanding detection algorithm will not operate for other disturbances on the system. As a result, passive methods suffer from large NDZ.

Regarding the passive islanding detection methods, over/under voltage and frequency (OVP/UVP and OFP/UFP) is the simplest method used for islanding detection. The IEEE Std. 1547 identifies the thresholds for both the voltage and frequency and the time delay required [5]. Unfortunately, if the load and generation on the island are closely matched, the change in voltage and frequency might be very small

Abbreviations: DG, distributed generation; TLS-ESPRIT, total least square-estimation of signal parameters via rotational invariance techniques; NDZ, non-detective zone; AFD, active frequency drift; SMFS, slip mode frequency shift; THD, total harmonic distortion; FFT, fast Fourier transform; OVP/UVP, over/under voltage; OFP/UFP, over/under frequency

* Corresponding author at: E&CE Department, University of Waterloo, 200 University Avenue West, Waterloo, Ont., Canada N2L 3G1.
Tel.: +1 519 888 4567x7060; fax: +1 519 746 3077.
E-mail address: hhmzeine@engmail.uwaterloo.ca (H.H. Zeineldin).

0378-7796/$ – see front matter © 2006 Elsevier B.V. All rights reserved.
doi:10.1016/j.epsr.2006.02.010

and within the IEEE standard specified thresholds, thus leading to an undetected islanding situation. In the phase jump detection method, the voltage waveform is compared with a reference waveform to determine the phase angle. If the phase angle exceeds the threshold value, an islanding condition is declared.

Total harmonic distortion (THD) of the DG voltage has been used as a means of islanding detection. If the system has nonlinear loads, the choice of a threshold for the THD becomes a tedious task [6,7]. The rate of change of frequency method overcomes some of the drawbacks of the previous methods but still fails when the load and DG capacity are closely matched. In [8,9], the rate of change of active power was proposed as a measure to detect islanding. The method is capable of differentiating between islanding and load switching conditions but unfortunately, it could fail under other disturbances such as voltage sag due to a short circuit or for a load to generation ratio on the island almost equal to unity. In [10,11], the ratio of frequency variation to load variation was used as a measure of islanding. Similarly, the method suffers from a NDZ.

To enhance the performance of islanding detection methods and decrease the NDZ, several methods have been proposed which use more than one parameter to detect islanding. In [12], both the rate of change of voltage and change in power factor were used to detect islanding. In [13], islanding was detected using the voltage unbalance and the THD of the DG current. In [14], both reactive and active power variation are used as means for islanding detection.

Two types of DG technology are commonly used for DG applications: inverter based and rotating machine technology. This paper proposes a new passive islanding detection method for DG of the synchronous type. Two new parameters, the frequency of oscillation and the damping factor of the generator's output frequency, are extracted using the TLS-ESPRIT algorithm. By analyzing the characteristics of the dominant modes in the DG output frequency signal, an islanding condition could be distinguished from a non-islanding one.

The paper is organized as follows: Section 2 provides the theory of the TLS-ESPRIT algorithm. Section 3 presents the proposed islanding detection method. The system model and data generation are presented in Section 4. Section 5 provides the simulation results. The last section draws the conclusions.

2. TLS-ESPRIT

The estimation of signal parameters via rotational invariance techniques (ESPRIT) has proven to be a powerful tool for extracting unknown parameters [15]. ESPRIT belongs to the class of signal subspace methods, which rely on eigendecomposition of the sample covariance matrix. This method yields high accuracy and can be applied to wide variety of problems including accurate detection and estimation of ciscoids (damped sinusoids). In this paper the TLS-ESPRIT algorithm, which is a modified version of the ESPRIT algorithm is used to extract signal parameters from the frequency waveform. The TLS-ESPRIT algorithm was introduced and analyzed in [15,16]. TLS-ESPRIT combines a reasonable computational complexity with a good modeling accuracy. Theory and application of the TLS-ESPRIT algorithm are presented in the next subsections.

2.1. Theory

The TLS-ESPRIT algorithm decomposes the signal into a group of damped sinusoids of different frequencies. The algorithm estimates the frequency, damping coefficient, amplitude and initial phase of each component of the signal. The model for the signal to be resolved by the TLS-ESPRIT is given by

$$x(n) = \sum_{i=1}^{M} h_i S_i[n] + \eta[n] \tag{1}$$

where

$$S_i[n] = \mathrm{e}^{c_i n} \tag{2}$$

$c_i = -\sigma_i + j\omega_i$ is the damping coefficient and frequency of oscillation of the ith signal component, M the modal order which represents the number of sinusoids representing a signal, η the noise signal and h_i is the complex amplitude of the ith signal component:

$$h_i = |h_i|\mathrm{e}^{j\vartheta} \tag{3}$$

Given N snapshots of the transient signal, $x(n), \ldots, x(n-N)$, then

$$\begin{pmatrix} x(n) \\ x(n-1) \\ \vdots \\ x(n-N) \end{pmatrix} = \begin{pmatrix} 1 & \cdots & 1 \\ \mathrm{e}^{-c_1} & \cdots & \mathrm{e}^{-c_M} \\ \mathrm{e}^{-Nc_1} & \cdots & \mathrm{e}^{-Nc_M} \end{pmatrix} \begin{pmatrix} h_1\,\mathrm{e}^{c_1 n} \\ h_2\,\mathrm{e}^{c_2 n} \\ \vdots \\ h_M\,\mathrm{e}^{c_M n} \end{pmatrix} + \begin{pmatrix} \eta(n) \\ \eta(n-1) \\ \vdots \\ \eta(n-N) \end{pmatrix} \tag{4}$$

The signal to be analyzed is modeled by a complex k-dimensional vector $a(c_i)$, which is called the steering vector:

$$a(c_i) = [1, \mathrm{e}^{-c_i}, \ldots, \mathrm{e}^{-Nc_i}]^{\mathrm{T}} \tag{5}$$

The k complex amplitudes are collected in a complex vector $s(n)$:

$$s_i = h_i\,\mathrm{e}^{c_i n} \tag{6}$$

From (4)–(6)

$$y = [a(c_1), a(c_2), \ldots, a(c_M)]S + \eta = AS + \eta \tag{7}$$

where $y = [x(n)x(n-1), \ldots, x(n-N)^{\mathrm{T}}]$, and $S = [s_1, s_2, \ldots, s_m]$.

Let y_1 and y_2 be two subarrays of y

$$y_1 = [a(c_1), a(c_2), \ldots, a(c_M)]S + \eta_1 = AS + \eta_1 \tag{8}$$

$$y_2 = [a(c_1)\mathrm{e}^{-c_1}, a(c_2)\mathrm{e}^{-c_2}, \ldots, a(c_M)\mathrm{e}^{-c_m}]S + \eta_2 = A\phi S + \eta_2 \tag{9}$$

where

$$\phi = \text{diag}[e^{-c_1}, e^{-c_2}, \ldots, e^{-c_M}] \tag{10}$$

Φ is a matrix that relates the measurements from a subarray y_1 to those of subarray y_2. From (8) and (9):

$$y = \begin{bmatrix} y_1 \\ y_2 \end{bmatrix} = \overline{A}S + \begin{bmatrix} \eta_1 \\ \eta_2 \end{bmatrix} \tag{11}$$

where

$$\overline{A} = \begin{bmatrix} A \\ A\phi \end{bmatrix} \tag{12}$$

The structure of the matrix $\overline{A}$ is analyzed to obtain estimated values of the diagonal elements of Φ without having to know A. TLS-ESPRIT requires the data to be separated into two orthogonal subspaces namely, the signal subspace and the noise subspace. The eigendecomposition of the covariance matrix R_{yy} can accomplish this task. Assuming the noise is white stationary:

$$R_{yy} = E\{y(n)y^*(n)\} = AR_{ss}A^* + \sigma^2 I \tag{13}$$

where E denotes expectation, R_{ss} the covariance matrix of the signals, and σ^2 is the noise variance. The eigendecomposition of the autocorrelation matrix can be placed in the form (14):

$$R_{yy} = E\lambda E^{*\text{T}} = E_s\lambda_s E_s^{*\text{T}} + E_{\text{noise}}\lambda_{\text{noise}}E_{\text{noise}}^{*\text{T}} \tag{14}$$

A signal subspace E_s defined in (14) can be estimated from the data. Since A and E_s span the same signal subspace, there exist a linear transformation T that relates A to E_s such that

$$E_s = \begin{bmatrix} E_x \\ E_y \end{bmatrix} = \begin{bmatrix} AT \\ A\phi T \end{bmatrix} \tag{15}$$

From (16), it can be seen that

$$E_x = E_y(T^{-1}\phi T) = E_y\psi \tag{16}$$

$$\psi = T^{-1}\phi T \tag{17}$$

Eqs. (16) and (17) are the main equations of ESPRIT algorithm. Eq. (16) represents a set of linear equations that can be solved for ψ. Eq. (17) represents the eigenvalue decomposition of ψ. Φ is the diagonal matrix of eigenvalues and γ is the matrix of eigenvectors of ψ. Solving (16) and (17) gives the required solution for Φ. The values of E_y and E_x can be estimated directly from the data by using the SVD technique but the estimated values $\hat{E}_y$ and $\hat{E}_x$ do not exactly satisfy (15). To account for this fact the total least square solution for (16) can be obtained by minimizing the following cost function:

$$\min \left\| \begin{bmatrix} \hat{E}_x \\ \hat{E}_y \end{bmatrix} - \begin{bmatrix} A \\ A\phi \end{bmatrix} T \right\|^2 \tag{18}$$

2.2. Application

To illustrate the performance of the TLS-ESPRIT algorithm, the algorithm was tested on well-defined functions and its performance is compared with the fast Fourier transform (FFT) method. The first signal, S_1, analyzed is a pure sine wave with a frequency of 30 Hz and zero damping factor, thus containing one mode. The singular values on the diagonal of the diagonal matrix obtained when calculating the singular value decomposition (SVD) of the autocorrelation matrix in the TLS-ESPRIT algorithm are [100.5, 100, 0, 0, . . ., 0]. The diagonal matrix of the SVD of the autocorrelation gives an indication of the number of modes in the signal. The first two values in the diagonal matrix, when converted to frequency values, correspond to the ±30 Hz and the rest are zeros indicating that there is no other modes in the signal. When FFT was applied to the same signal, an impulse signal at 30 Hz was obtained.

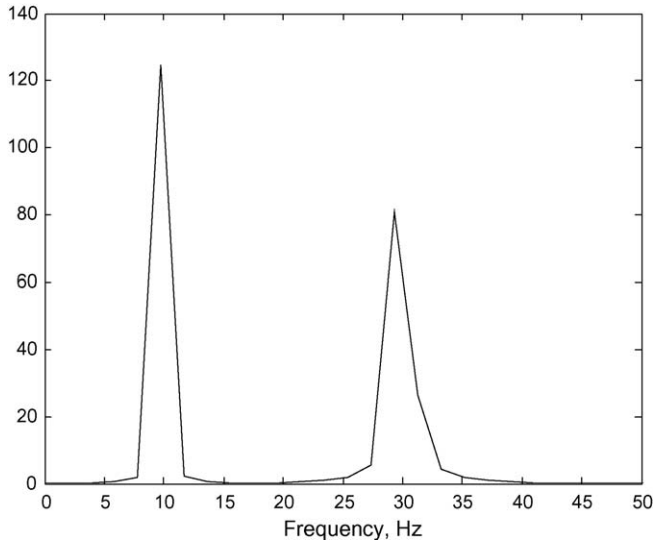

Fig. 1. FFT output for signal S_2.

A 10 Hz component with zero damping was added to S_1 to give a new signal S_2. The diagonal values obtained are [101,100, 100, 100, 0, 0, . . ., 0]. The output indicates that there are two modes in the signal which when converted to frequencies correspond to the 10 and 30 Hz components. Similarly, FFT resulted in two impulse signals at the 10 and 30 Hz components as shown in Fig. 1.

A sine wave that has two damped sinusoidal components, 30 Hz with a damping factor of 50 and 10 Hz with a damping factor of 20 and is denoted as S_3, was applied to TLS-ESPRIT algorithm. The diagonal matrix obtained was [3.5455, 0.7776, 0.0021, 0.002, 0, . . ., 0] which indicates that the signal has two modes corresponding to the two components in the signal. Fig. 2 shows the FFT of signal S_3. The FFT spectrum shows peaks at the 10 and 30 Hz. Due to the damping factors, which were multiplied by the sinusoidal components, the spectrum is no longer impulsive at the 10 and 30 Hz.

The last signal S_4 analyzed was a sine wave composing of two components of frequency 10 Hz, damping 20 and 11 Hz with damping 50 but with additive white noise of 1%. The diagonal matrix obtained is [2.258, 0.4924, 0.0018, 0.0017, 0, 0, . . ., 0]. Figs. 3 and 4 show the output modes of the signal analyzed using TLS-ESPRIT and FFT, respectively.

It can be seen from Fig. 3 that TLS-ESPRIT is powerful in estimating and extracting damped sinusoids with additive noise.

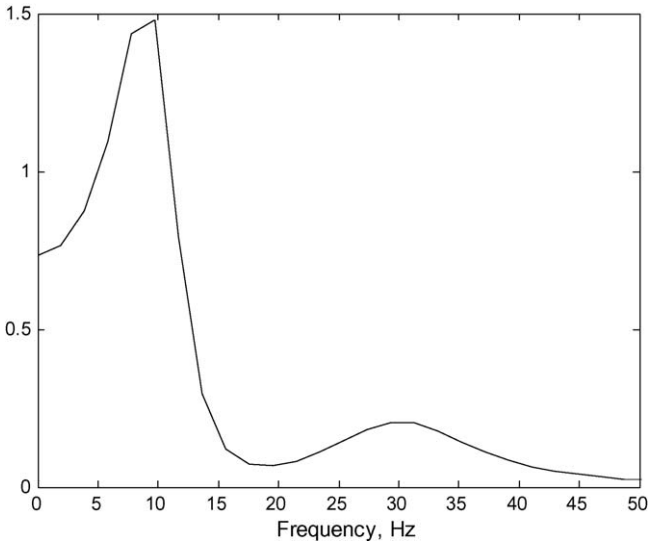

Fig. 2. FFT output for signal S_3.

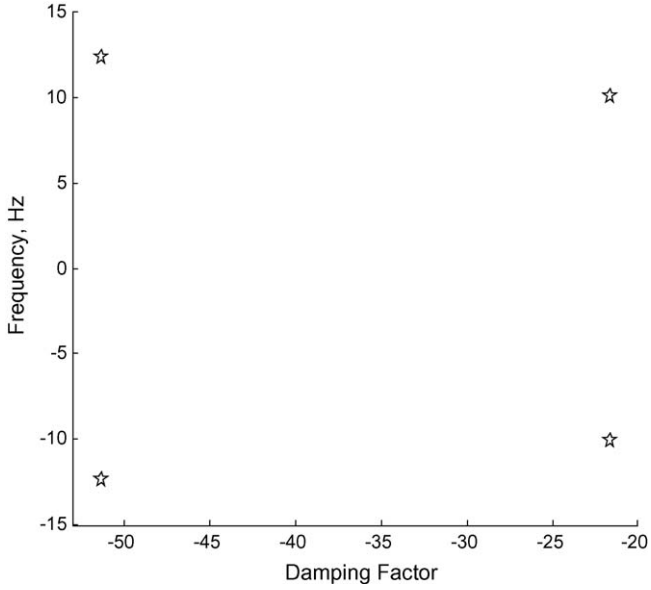

Fig. 3. TLS-ESPRIT output for signal S_4.

On the contrary, from Fig. 4, the damped 10 and 11 Hz components cannot be differentiated when using FFT, thus making TLS-ESPRIT superior in analyzing damped sinusoids. Besides that, TLS-ESPRIT is capable of extracting accurately the damping factor, which is one of the parameters to be used in the proposed islanding detection method.

3. Proposed islanding detection method

This section presents the proposed passive islanding detection method. The frequency of oscillation and the damping factor of the DG output frequency are two new parameters used to detect islanding. Prior to presenting the proposed algorithm, a mathematical proof is presented to show the effectiveness and the applicability of these two parameters in detecting islanding.

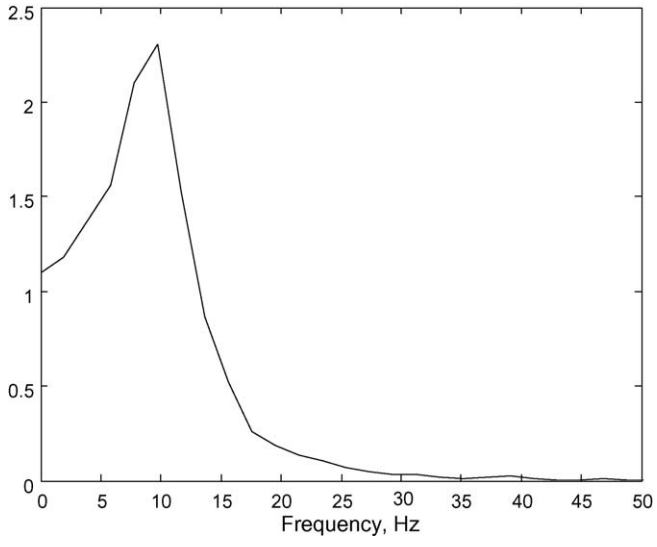

Fig. 4. FFT output for signal of S_4.

3.1. Mathematical proof

A power system is subjected to numerous random power disturbances from sudden application or removable of loads, capacitor switching, short circuit, etc. Each disturbance will be followed by a power swing. The equation of motion (Swing equation) for a synchronous machine connected to an infinite bus is given by

$$\frac{2H}{\omega_0}\frac{\mathrm{d}^2\delta}{\mathrm{d}t^2} = P_\mathrm{m} - P_\mathrm{e} \tag{19}$$

where H is the machine inertia constant, ω_0 the angular synchronous speed, P_m and P_e the mechanical power and electrical power, respectively, and δ is the rotor angle [17]. In small perturbation studies of a synchronous machine and at a certain frequency of oscillation, the machine braking torque can be analyzed into two components: the damping component in phase with the machine rotor speed deviation, and the synchronizing component in phase with the rotor angle deviation. The simplified second order system block diagram is shown in Fig. 5 and

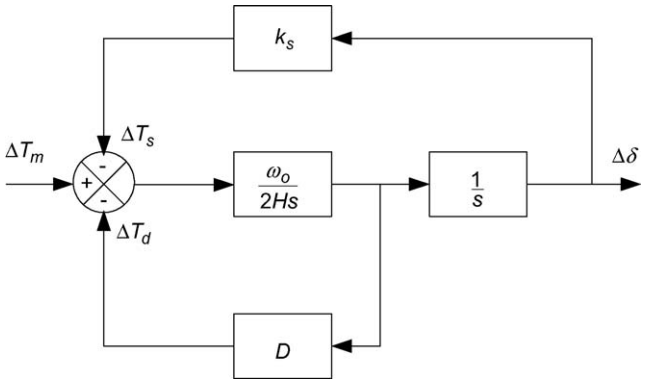

Fig. 5. Second-order system block diagram.

the characteristic equation can be written as follows [18]:

$$s^2 + \frac{\omega_0 D}{2H}s + \frac{\omega_0 k_s}{2H} = 0 \quad (20)$$

The two roots of (20) are

$$\lambda_{1,2} = -\frac{\omega_0 D}{4H} \pm j\omega_d, \quad \omega_d = \left(\frac{\omega_0 k_s}{2H} - \frac{\omega_0^2 D^2}{16H^2}\right)^{0.5} \quad (21)$$

where D is the damping coefficient and k_s is the synchronizing coefficient.

Using the simplified second order system, it can be seen from (21) that with the DG operating in parallel with the utility, the DG output frequency oscillates with a frequency ω_d and has a certain damping factor. For an islanded synchronous DG, there will be no synchronizing torque and k_s will equal zero. In this case, the roots in (21) become

$$\lambda_{1,2} = -\frac{\omega_0 D}{2H} \quad \text{and} \quad 0 \quad (22)$$

and the frequency deviation during an islanded condition can be expressed as follows [19]:

$$\Delta f = \frac{\Delta P}{D}(1 - e^{(-\omega_0 D/2H)t}) \quad (23)$$

By comparing (21) and (22), it can be seen that the response of the DG varies depending on whether the DG is connected to the grid or not. Two significant differences can be identified:

1. With the DG operating in parallel, the DG output frequency has both a frequency and damping component as imposed to just a damping component in case of islanding.
2. The damping component in case of DG islanding is greater than the damping component in case of DG parallel operation.

The frequency of oscillation and the damping factor of the DG output frequency are extracted using TLS-ESPRIT algorithm. Thresholds are chosen to distinguish between an islanding and a non-islanding situation.

3.2. Proposed algorithm

Since the frequency of oscillation of DG output frequency is small when a DG is exposed to a disturbance, a large window size for analyzing the signal will be required to accurately model the waveform. Thus, islanding will not be detected within the standard allowable time. In order to avoid this problem, a smaller window size is taken (350 ms) and in this case the modes of the signal are analyzed irrespective of the damping and frequency of oscillation values. If all modes have no frequency component and have a damping factor, this indicates that there is a monotonic increase or decrease in the signal, which is the case when islanding occurs. Analyzing the modes in the signal provides a mean of identifying the pattern of the signal. Fig. 6 presents the proposed islanding detection algorithm.

The algorithm starts by calculating the frequency and damping factor for each mode within the DG output frequency signal.

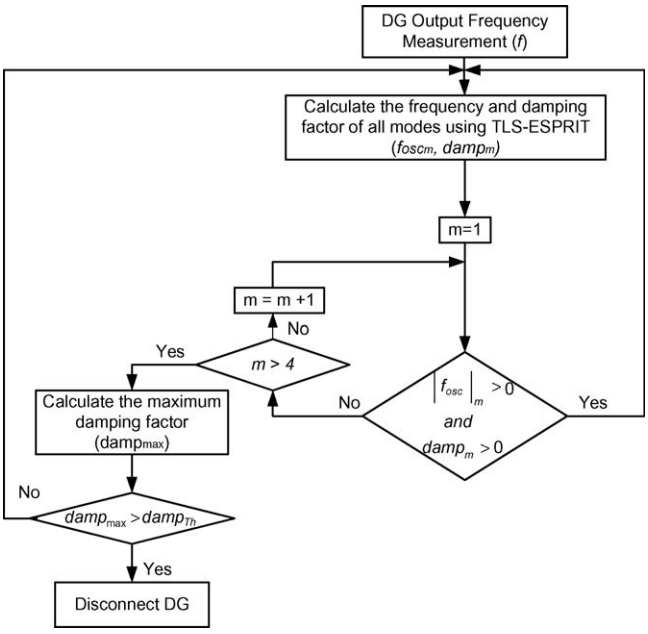

Fig. 6. Proposed islanding detection algorithm.

If one of the modes in the signal has a frequency component, this indicates that the DG is operating in parallel with the utility and there is no need to go through the other modes. If the frequency and damping component of a mode are not simultaneously greater than zero, the mode number is updated to check the next node's frequency and damping component. This is repeated until all modes are checked. If all the modes have been tested and all do not satisfy the previously mentioned condition, the mode with the maximum damping factor is determined and its damping factor is stored as $\text{damp}_{\max}$ and compared with a threshold value. The threshold on the damping factor is to assure that the algorithm does not misoperate for normal conditions (both f_{osc} and $\text{damp}_{\max}$ are equal to zero). It should be noted that the two new parameters are used in conjunction with the OVP/UVP and OFP/UFP to reduce the NDZ.

The parameters m, f_{oscm}, damp_{m}, $\text{damp}_{\max}$ and damp_{T} represent the mode number in the signal, the frequency of oscillation, damping factor of mode m, the maximum damping factor in all modes of a signal and the threshold on the damping factor, respectively.

4. System model

The system under study is the IEEE 34-bus system shown in Fig. 7. A 1 MW synchronous DG is connected through a 1 MVA transformer at node 848 with a local load. The excitation and governor control of the DG adopted are given in [20].

In order to design an efficient islanding detection algorithm, different common disturbances have been created on the system. The cases studied include:

1. Capacitor switching
2. Short circuit (3-ph and single line to ground)

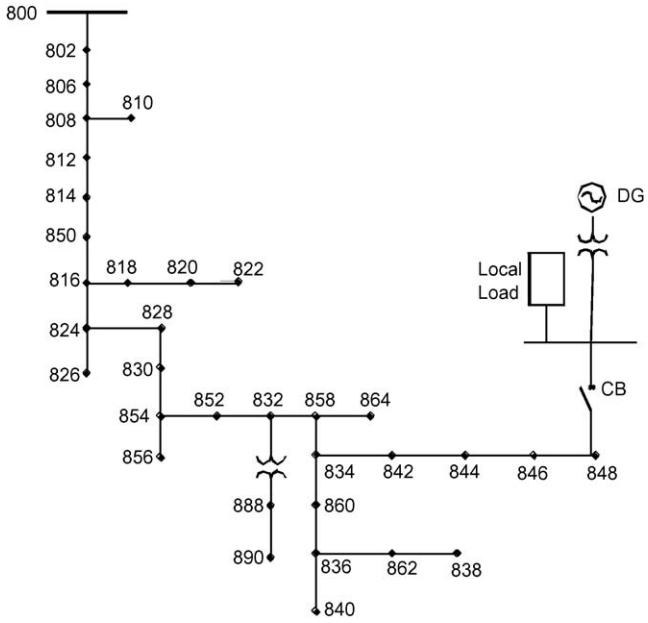

Fig. 7. IEEE 34-bus system.

3. Load change
4. Islanding of the DG

The waveforms are generated using the PSCAD/EMTDC software. Table 1 presents a list of all the cases generated and the varying conditions associated with each case.

For each case, samples of the generated frequency waveforms from the PSCAD/EMTDC are presented. The waveforms are then analyzed by the TLS-ESPRIT algorithm to extract the damping factor and the frequency of oscillation of the signal components. The extracted parameters are then applied to proposed islanding detection algorithm.

4.1. Capacitor switching

In a distribution power system, transients are initiated by the switching of shunt capacitor banks in the system. These transients propagate and can be sensed at other locations far from the capacitor. In order to take into account capacitor switching, capacitors of ratings 0.3, 0.45, 0.9, 1.8, and 2.7 Mvar were switched at different nodes on the system. Fig. 8 shows the output frequency of the DG when capacitors, with different Mvar ratings, are switched, for example, at node 840.

The amplitude of the oscillation in frequency increases as the Mvar rating of capacitor increases. The frequency oscillates and damps until it reaches its nominal value. The nature

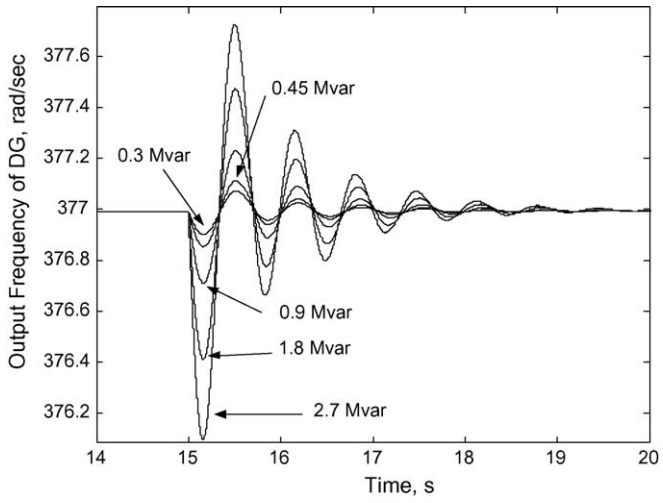

Fig. 8. Effect of capacitor switching on the generator's output frequency.

of the waveforms obtained is a damping sinusoid waveform. TLS-ESPRIT is suitable for decomposing such waveform into a group of damped sinusoids.

4.2. Short circuit

Faults on the distribution power system are another source of disturbances that can cause nuisance tripping of the islanding detection algorithm. During the short circuit, the point at which the DG is connected experiences voltage sag that might exceed the undervoltage threshold, leading to incorrect operation of the DG circuit breaker. To account for short circuit currents when designing the islanding detection algorithm, 3-ph, 2-ph and 1-ph to ground faults were applied at different nodes on the system. Fig. 9 presents the output frequency of the DG when a 3-ph and 1-ph fault occurs at node 840.

For both 3-ph and 1-ph faults, the output frequency of the DG oscillates and damps until it reaches its nominal value. Similarly, TLS-ESPRIT is suitable for analyzing and extracting the frequency of oscillation and the damping factor of such waveforms.

4.3. Load change

Load change is one of the most common disturbances that occur on a distribution network that has an effect on the frequency of the DG. Loads in the range of 450 kW–1 MW with power factors ranging from 0.5 lagging to unity have been switched at different nodes on the distribution system. Fig. 10 presents four cases where a varying load at node 858 was

Table 1
Data generated

Cases	Varying conditions
Capacitor switching	0.3, 0.45, 0.9, 1.8, and 2.7 Mvar capacitors switched at different nodes on the system
Short circuit	1-ph, 2-ph, and 3-ph to ground faults at different nodes on the system
Load change	450 kW–1 MW loads including nonlinear loads are switched at different nodes on the system
Islanding	Islanding with loads greater, almost equal and less than the DG rating

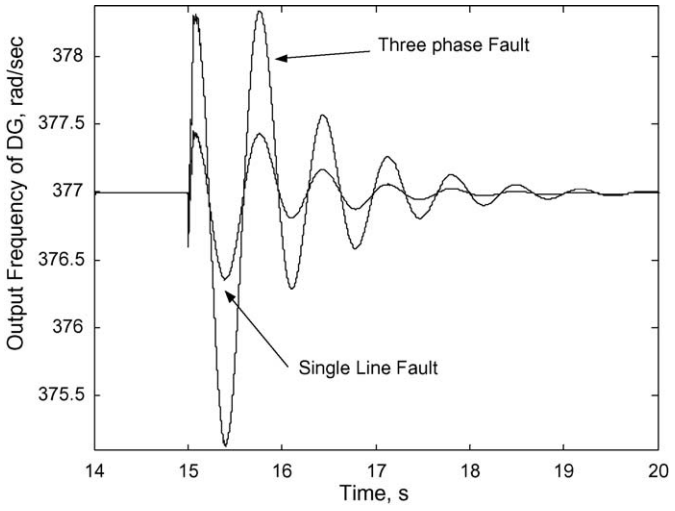

Fig. 9. Effect of short circuit on the generator's output frequency.

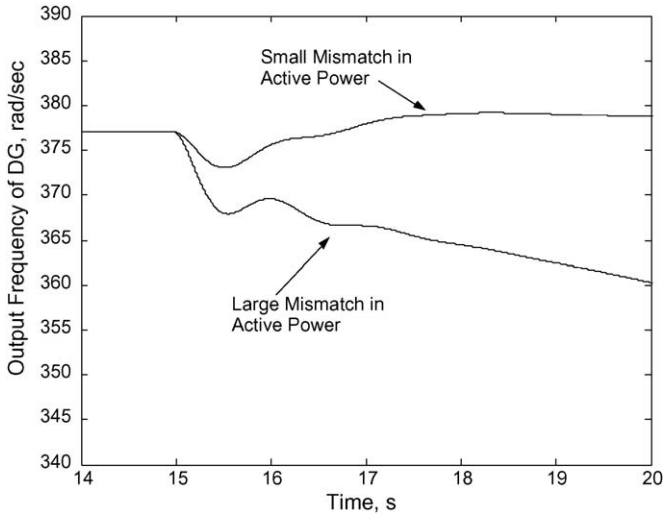

Fig. 11. Effect of islanding on the generator's output frequency.

switched. When the load is switched on, the frequency oscillates and then slowly damps until the steady state frequency is reached. TLS-ESPRIT could accurately be used to model the waveforms obtained below.

4.4. Islanding

The main objective is to accurately distinguish between islanding and non-islanding cases to eliminate nuisance tripping of the islanding protection detection algorithm. The response of the DG frequency was observed for different island loading conditions. Fig. 11 shows the frequency of the DG when islanding occurs for a small and large mismatch in loadings on the island. It can be seen that for some cases, where there is a significant difference between the load and generation on the island, islanding could be easily detected using OFP/UFP.

When the load and generation on the island are almost equal, the OFP/UFP method will fail to detect islanding. Additional parameters need to be measured to work in parallel with the OFP/UFP to prevent undetectable islanding conditions. The threshold set for these additional parameters should be capable of distinguishing between islanding and disturbance conditions. Comparing Fig. 11 to Figs. 8–10, it can be observed that the DG output frequency responds differently, when a disturbance occurs while the DG is connected to the utility, and when the DG is islanded. The figures show two distinguishing features, which are the damping and frequency of oscillation of the DG frequency. During disturbances and islanding conditions, the frequency varies and damps until it reaches a steady state value. The frequency of oscillation and the damping factor in the output frequency waveform of the DG are the two new parameters that are used in islanding detection and are extracted using TLS-ESPRIT.

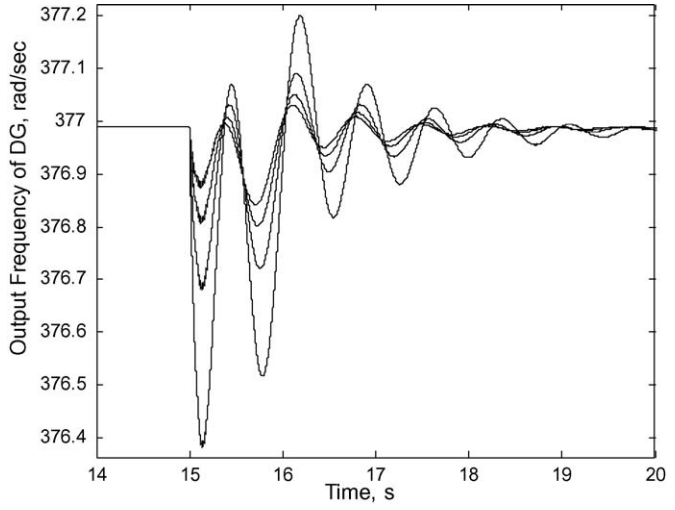

Fig. 10. Effect of load change on the generator's output frequency.

5. Simulation results

The IEEE 34-bus system under study is simulated on the PSCAD/EMTDC software and is subjected to the different aforementioned disturbances. The frequency waveform is measured and is applied to the TLS-ESPRIT algorithm, which was programmed on MATLAB. A sampling time of 500 μs was used and each signal was represented by four modes, which was determined based on the S matrix diagonal values. To illustrate the performance of the TLS-ESPRIT in identifying the modes of the DG output frequency signal, a sample of the different disturbances is applied to the algorithm. Fig. 12 presents the simulation results obtained using TLS-ESPRIT.

It can be seen that non-islanding cases are characterized by modes containing damping and other modes contain both damping and frequency. On the other hand, all the modes in case of an islanding situation do not contain any frequency but have a damping factor. The modes estimated using the TLS-ESPRIT consent with the mathematical proof presented in Section 3. Since a small window was taken for calculating the modes of the frequency signal, the numerical values obtained from the TLS-ESPRIT algorithm will not correspond to the values calculated using (21) and (22). The characteristics of the modes

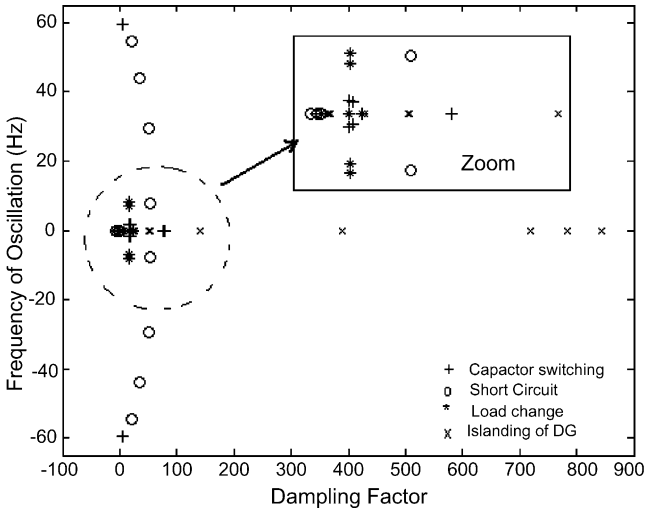

Fig. 12. Simulation results obtained using TLS-ESPRIT.

were used as a significant measure to distinguish between an islanding and a non-islanding case to detect islanding accurately. Aside from that, the simulation results show that islanding cases have large damping factors. Thus, by examining the nature of the modes and setting a threshold on the damping factor, DG islanding of synchronous DG could be detected with negligible NDZ.

6. Conclusion

This paper presented a new passive islanding detection algorithm for synchronous DG. The algorithm is based on two new parameters for islanding detection, the frequency of oscillation and the damping factor of the DG frequency output. The TLS-ESPRIT algorithm was capable of accurately extracting the modes in the DG output signal. Examining the characteristics of the resulting modes could distinguish an islanding condition from a non-islanding one, thus providing accurate islanding detection. A significant advantage of the proposed islanding detection method is its negligible NDZ. The simulation results consent with the mathematical proof presented in this paper.

Acknowledgement

The authors gratefully acknowledge Prof. Hussein M. Zein El-Din for his fruitful discussion.

References

[1] H. Kobayashi, K. Takigawa, E. Hashimoto, Method for preventing islanding phenomenon on utility grid with a number of small scale PV systems, in: Proceedings of the IEEE Photovoltaic Specialist Conference, vol. 1, October 1991, pp. 695–700.

[2] M. Ropp, M. Begovic, A. Rohatgi, Analysis and performance assessment of the active frequency drift method of islanding prevention, IEEE Trans. Energy Conversion 14 (3) (1999).

[3] G.A. Smith, P. Onions, D. Infield, Predicting islanding operation of grid connected PV inverters, IEE Proc. Electric Power Appl. 147 (2000) 1–6.

[4] G. Hung, C. Chang, C. Chen, Automatic phase shift method for islanding detection of grid connected photovoltaic inverters, IEEE Trans. Energy Conversions 18 (1) (2003).

[5] IEEE Std. 1547-2003, IEEE Standard for Interconnecting Distributed Resources with Electric Power Systems, 2003.

[6] M. Ropp, W. Bower, Evaluation of islanding detection methods for photovoltaic utility interactive power systems, International Energy Agency Implementing agreement on Photovoltaic Power Systems, Tech. Rep. IEA PVPS T5-09, March 2002.

[7] G.A. Kern, Sunsine300, utility interactive ac module anti islanding test results, in: Proceedings of the IEEE Photovoltaic Specialist Conference, September 1997, pp. 1265–1268.

[8] M. Redfern, O. Usta, G. Fielding, Protection against loss of utility grid supply for a dispersed storage and generation unit, IEEE Trans. Power Del. 8 (3) (1993).

[9] M. Redfern, O. Usta, A new microprocessor based islanding protection algorithm for dispersed storage and generation units, IEEE Trans. Power Del. 10 (3) (1995).

[10] S. Huang, F. Pai, Design of an islanding detection circuit for dispersed generators with self commutated static power converters, in: Proceedings of the IEEE Power Electron. Specialist Conference, vol. 2, June 2000, pp. 668–673.

[11] F. Pai, S. Huang, A detection algorithm for islanding prevention of dispersed consumer owned storage and generating units, IEEE Trans. Energy Conversion 16 (4) (2001).

[12] S. Salman, D. King, G. Weller, New loss of mains detection algorithm for embedded generation using rate of change of voltage and change in power factor, in: Proceedings of the IEE Development in Power System Protection, April 2001, pp. 82–85.

[13] S. Jang, K. Kim, An islanding detection method for distributed generations using voltage unbalance and total harmonic distortion of current, IEEE Trans. Power Del. 19 (2004) 745–752.

[14] C. Jeraputra, P. Enjeti, I. Hwang, Development of a robust anti-islanding algorithm for utility interconnection of distributed fuel cell powered generation, in: Proceedings of the IEEE Applied Power Electronics Conference and Exposition, vol. 3, February 2004, pp. 1534–1540.

[15] R. Roy, T. Kailath, Esprit estimation of signal parameters via rotational invariance techniques, IEEE Trans. Acoustics, Speech Signal Process. 37 (7) (1989) 984–995.

[16] R. Roy, A. Paulraj, T. Kailath, ESPRIT—a subspace rotation approach to estimation of parameters of cisoids in noise, IEEE Trans. Acoustics, Speech Signal Process. ASSP-34 (5) (1986).

[17] P.M. Anderson, A.A. Foud, Power System Control and Stability, 1st ed., The Iowa State University Press, 1977.

[18] H.M. Zein El-din, An efficient approach for dynamic stability analysis of power systems including load effects, Ph.D. Thesis, Faculty of Engineering, McMaster University, Hamilton, Ontario, Canada, June 1978.

[19] W. Elmore, Protective Relaying Theory and Applications, ABB Power T&D Company Inc., 1994.

[20] K. Okuyama, T. Kato, Y. Suzuoki, T. Funabashi, K. Wu, Y. Yokomizu, T. Okamoto, Improvement of reliability of power distribution system by information exchange between distributed generation-sharing of all DG's information, in: Proceedings of the IEEE Power Engineering Society 2001 Summer Meeting, vol. 1, 2001, pp. 468–473.